Dynamic Modeling and Mitigation of Cascading Failures in Power Grids with Interdependent Cyber and Physical Layers

Sina Gharebaghi, *Student Member, IEEE,* Nilanjan Ray Chaudhuri, *Senior Member, IEEE,* Ting He, *Senior Member, IEEE,* and Thomas La Porta, *Fellow, IEEE*

***Abstract*—Modeling and prevention of cascading failure in power systems are important topics of research. We propose a dynamic cascading failure model that considers realistic interdependencies between power and communication networks used for system monitoring and control in power grids. In this model, power line outages do not immediately disconnect communication links, whereas communication nodes have battery backup that starts depleting after considerable load shedding in the collocated bus or bus outage. When a communication node's battery is fully depleted, the node disconnects from the cyber layer, potentially reducing the observability and controllability of the power grid. A centralized optimal preventive controller (OPC) to minimize load shedding is proposed for cascade mitigation, which is applied selectively on fully observable and controllable islands. The OPC considers AC power flow equations, multiple hard constraints, and treats overloading of lines as soft constraints. The results of Monte-Carlo simulations on the IEEE 118-bus and the $2,383$-bus Polish systems demonstrate that the proposed OPC is effective in mitigating cascading failures. Finally, we demonstrate that our recently proposed Backward Euler method with Predictor-Corrector can reduce the average simulation time by approximately 9 – 26-folds compared to the Trapezoidal method with acceptable accuracy.**

***Index Terms*—Cascading failure, Dynamic model, Cyber-physical power grid, Optimal preventive control, Trapezoidal and Backward Euler methods.**

I. Introduction

DUE to the complexity and interdependence of power system and communication network for system monitoring and control, it is important to develop methods for predicting and mitigating the impact of coupled cascading failures in such cyber-physical systems. One such approach is the development of time-domain simulation tools that can accurately model the behavior of coupled power and communication systems under various contingencies, and conducting statistical analysis for cascading failures with different initial outages.

The ground truth for cascading failures in such complicated networks can only be obtained through a detailed dynamic model involving a set of nonlinear differential and algebraic equations (DAEs). However, studying cascading failures in cyber-physical systems like power grids is challenging since it requires long-term simulations that go beyond typical planning studies lasting only around $\approx 20 - 30$ s. Due to computational complexity such studies have been proven to be elusive, and have forced the research community to use Quasi-Steady-State (DC-QSS, AC-QSS) models [1], which despite recent improvements [2], cannot capture many of the phenomena in the dynamic models [3].

The primary goals of this paper are the formulation of a dynamic model for complex power grids incorporating the realistic interdependent cyber and physical networks therein, and the development of an effective methodology for optimally mitigating cascading failures in such grids. Furthermore, we aim to employ an efficient time-domain simulation approach that facilitates statistical analysis of such complex models.

A. Literature on Cascading Failure in Cyber-Physical Grids

Despite the significant research interest in cascading failure of the physical layer of power systems, only a few papers [4]–[13] have addressed the unique challenges posed by representing cascading failure in the interdependent cyber and physical layers of power grids. To the best of our knowledge, none of these works [4]–[13] consider a dynamic model, which represents the realistic behavior of power systems.

(1) Modeling of cascading failure in cyber-physical power grids: The purpose of papers [4], [6] is to examine how interdependencies and structural characteristics of communication networks impact cascading failures in power grids. The authors found that increasing interdependency leads to a greater robustness against cascading failures. In [7], [8], stochastic models of cascading failures are proposed that consider the interdependency between cyber and physical layers of power networks. The authors of [9] studied the effects of wind power uncertainty and penetration levels on the vulnerability of an interdependent system to cascading failures. An interdependent Markov-chain framework was proposed in [10] and tested to study cascading failures in power systems. References [4], [9] used DC-QSS models, whereas [6] used AC-QSS models. References [7], [8] have used approximated linearized PF. The authors of [11], [12] proposed DC-QSS model for cascading failure simulation and control in coupled power-communication systems.

Using a DC-QSS model in [13], authors highlight that large-scale cascading failures in power systems can lead to outages in the interconnected communication network, disrupting the monitoring and control of the power system. Reference [5] addresses the challenge of topology estimation in power

Authors are with The School of Electrical Engineering and Computer Science, The Pennsylvania State University, University Park, PA 16802, USA. e-mail: svg5765@psu.edu, nuc88@engr.psu.edu, tzh58@psu.edu, and tfl12@psu.edu.

Financial support from NSF Grant Award ECCS 1836827 is gratefully acknowledged.

grids that involve interconnected cyber and physical networks, particularly in the context of cascading failures. The authors formulate two optimization problems to tackle this issue: one for island estimation and another for line outage detection in the estimated island. It is worth noting that although the model is primarily based on the DC-QSS model, the authors have also conducted testing and verification using the AC power flow model.

Regarding the interdependency modeling in existing literature [4]–[13], different types of stochastic interconnections between the physical and cyber layers of power grids have been considered in [4], [6], [7], [9], [10], [13]. Another group [5], [8], [11], [12] examines deterministic modeling of interdependencies under certain assumptions. For instance, in [8], authors assume that the failure of a communication node leads to the failure of the corresponding power node, as the power node cannot receive information from the control center. Similarly, when a power node fails, the corresponding communication node fails. On the other hand, studies by [5], [11], [12] assume that an outage of a power bus causes the outage of corresponding communication node. However, it should be noted that an outage in the communication node does not directly result in a power bus outage; rather, it limits the controllability and observability of the system.

(2) Prevention of cascading failure in cyber-physical power grids: Papers [5], [11]–[13] propose optimal mitigation of cascading failure in power grids with interdependent cyber and physical layers. The authors of [11], [12] design a communication network for supervisory control and data acquisition (SCADA) system in a power grid consisting of power line carrier communication (PLCC) links and non-PLCC links (e.g., microwave) under a budget constraint with the aim of maximizing the demand served during coupled cascade propagation. Reference [13] proposes a preventive control approach based on optimal generation and load reduction using a modified DC optimal power flow (OPF), which takes into account a progressively reducing controllability due to communication failures. However the approach in [13] (also other papers) assumes accurate knowledge of the system topology (Y_{bus}), i.e., full observability of breaker statuses. To fill this gap, [5] performs topology estimation as the size of observable regions of islands and the number of observable breaker statuses continue to reduce over time. Additionally, [5] focuses on the impact of grid estimation on preventive control of cascading failure.

B. Gaps in Literature

The following are gaps in existing cascading failure models for power grids with interconnected cyber and physical layers:

1) *Physical layer model:* None of the existing works [4]–[13] consider dynamic models, which are necessary to accurately capture the ground truth during cascading failure.
2) *Cyber layer model:* In absence of dynamic models there is a lack of explicit representation of time. As a result, the temporal decay of battery backup has not been modeled in the literature, which is essential to determine the status of the communication nodes over time.
3) *Interdependency model:* In absence of realistic battery backup model described above, existing QSS-based models used probabilistic approaches to determine the status of communication nodes following outages in the cyber-physical systems.
4) *Preventive control model:* All preventive control methods found in the literature [5], [11]–[13] are based on DC-OPF which ignore the effect of reactive power flow. A realistic simulation of preventive control should consider: (i) collecting data required as inputs for the optimization problem, (ii) initiating calculation of optimal preventive control for the fully observable islands, (iii) considering the time-delay for convergence of the optimization problem, and (iv) applying these commands to actuators for fully controllable islands. Existing papers did not consider each of steps (ii)-(iv).

C. Contributions of This Work

This paper:

1) introduces a dynamic cascading failure model for power grids consisting of interdependent physical and cyber layers with fiber-optic/wireless communication systems supported by battery backup. This realistic model allows for a more accurate representation of the behavior and impacts of cascading failures in such complex systems.
2) considers a realistic interdependency model which takes into consideration battery backup with temporal depletion of battery energy.
3) proposes a centralized optimal preventive controller (OPC) designed to mitigate cascading failures in islands with full observability and controllability. Application of OPC in other islands can have a negative impact on cascade mitigation as described later. OPC problem takes into account AC power flow equations, multiple hard constraints, and line overloading as soft constraint. It considers all the realistic attributes mentioned under section I-B.
4) performs time-domain simulations of the dynamic model using our previously proposed BEM-PC approach [3], which is shown to significantly reduce the average simulation time compared to the traditional methods. Unlike [3], where only the physical layer considered, this work provides a more efficient tool for analyzing and evaluating dynamic cascading failures in coupled power and communication networks.
5) presents exhaustive simulation results on the IEEE 118-bus system and the $2,383$-bus Polish network that demonstrate the efficiency, applicability, and scalibility of the proposed model.

The proposed modeling and simulation framework is deterministic in nature and does not take into account aspects like probability of relay misoperation and breaker failure, which are left to future work.

II. Dynamic Model of Cascading Failure in Coupled Power & Communication Networks

A. Modeling of Physical Layer: Power Network

The physical layer in the dynamic model of cascading failure can be represented by a set of coupled nonlinear

DAEs and inequalities to account for discrete relay actions, as follows:

$$\dot{x} = f(x, V, z) \tag{1}$$

$$0 = I(x, V, z) - Y_N(z)V \tag{2}$$

$$0 \succ h(x, V, z). \tag{3}$$

where, the state vector of machines and the vector of real and imaginary parts of nodal voltages are denoted by x and V, respectively. The status of relays is indicated by a vector of binary variables z. The real and imaginary parts of injected currents at buses are represented by vector I while the real form of the network's admittance matrix is denoted by Y_N.

The proposed dynamic model for physical layer includes a fourth-order synchronous generator model with state variables $E_q^{'}$, $E_d^{'}$, δ, $\Delta\omega$, as well as first-order governor and static exciter models [14]. Both static constant power loads and dynamic representation of synchronous condensers are considered in the model. The synchronous condensers have similar models as generators, except that they lack governors. The model also includes appropriate relays, such as overcurrent (OC) relays, out-of-step machine protection, undervoltage load shedding (UVLS) relays, and pre-specified special protection schemes (SPSs). Further details on the modeling of physical layer of power grid can be found in section IV of [3].

B. Modeling of Cyber Layer: Communication Network

The cyber layer of power grid is composed of two primary networks: SCADA and wide-area monitoring, protection, and control (WAMPAC). SCADA utilizes redundant data measurements from remote terminal units (RTUs) for topology and state estimation, while WAMPAC uses phasor measurement units (PMUs) as sensors and is experiencing a rapid growth [5]. The WAMPAC's PMU-based sensing offers advanced power system monitoring and control functionalities, whereas SCADA systems are limited in this regard due to slower sampling rates ($\approx$ 4 s, see page 160 of [15]) of RTUs. As the cyber layer in power grid continues to evolve, it is crucial to recognize the strengths and limitations of each network and determine their appropriate use in ensuring efficient power grid operations. Due to its significant potential and continuous growth, this paper assumes WAMPAC network as part of the cyber layer modeling.

A typical cyber layer of a power grid consists of a control center (CC) connected to the communication nodes through wireless (usually microwave) and fiber-optic links. The communication nodes have different accessories including sensors, e.g., PMUs in our case, which draw power from the substations (i.e., buses) and are equipped with battery backup. The CC receives measurements, performs state estimation, and runs other algorithms for system operation. In our case, we focus on OPC running at the CC and sending commands through the communication network to generators and loads for power output reduction and load shedding. The topology of the communication network, the battery backup model, and the interdependency model are described next. Throughout the rest of the paper, we use 'bus' and 'node', respectively, to represent a node in the power and the communication network. Let $G_p = (V_p, E_p)$ and $G_c = (V_c, E_c)$ be the graphs representing the physical and the cyber layers of power grid, respectively, comprising bus set V_p, power line set E_p, nodes V_c, and communication links E_c.

1) Topology of Communication Network: In our work, the buses in G_p and the nodes of G_c are assumed to be collocated ($|V_p| = |V_c|$), and $|E_c|$ is a fraction of $|E_p|$, where $|\cdot|$ denotes cardinality of a set. It should be noted that our proposed cyber-physical cascading failure model is not limited to the specific communication network topologies described next. These topologies are just examples used for our studies.

In line with [13], the CC is situated at a bus with the highest betweenness centrality (BC) of G_p. To conduct a comprehensive study, we analyze various topologies for the communication network as follows:

- *Topology (1):* The minimum spanning tree of G_p is used as G_c, which is given by $G_c^1 = (V_c^1, E_c^1)$.
- *Topology (2):* The graph G_c^1 is a subgraph of this topology. Let us define the degree of redundancy in G_c as $\beta = \frac{|E_c|}{|E_p|}$. To construct the communication network for this topology with a given degree of redundancy β (higher than that of Topology (1)), we propose the following steps.
  Step (1): Create a replica of G_p and call it $G_c^0 = (V_c^0, E_c^0)$.
  Step (2): Determine the set of candidate links to be eliminated from G_c^0, which is given by $E_c^0 - E_c^1$. Then calculate the number of links to be eliminated from $E_c^0 - E_c^1$, which is given by $N_l^t = (1 - \beta) \times |E_c^0|$.
  Step (3): Sort the buses in G_c^0 based on their BC values from lowest to highest BC. Next, begin disconnecting the links that belong to the set $E_c^0 - E_c^1$ starting from the ones adjacent to the node with the lowest BC. Continue the process of disconnection for nodes with progressively higher BC values until the number of disconnected links become equal to N_l^t. The resulting graph serves as communication network G_c^2.

Since the number of available links is constrained, in Topology (2), we assign a progressively higher importance to nodes with higher BC values. The intuition behind this is that in the communication network, more information will pass through a node with higher BC. However, we do not claim any advantages or novelty in designing the communication network in this manner. It is simply an approach that gives us a given degree of redundancy β, which by no means is claimed to be optimal as that is not the focus of this paper. For our study, we made the assumption that all links in the communication network are either wireless communication links or fiber-optic channels, with backup power coming from battery energy storage system in the nodes. The realistic battery backup model is proposed in the following section.

2) Battery Backup for Communication Nodes: In this paper, we consider a realistic battery backup model with temporal depletion of battery energy for each node in the communication network. As mentioned earlier, each communication node is collocated with a bus and draws its power from the grid under normal condition. *It is important to note, in our model each load bus represents an aggregation of substations supplying aggregated loads. Therefore, the extent of load shedding experienced at a bus can indicate the severity of the outage and indirectly reflect the degree to which a multitude*

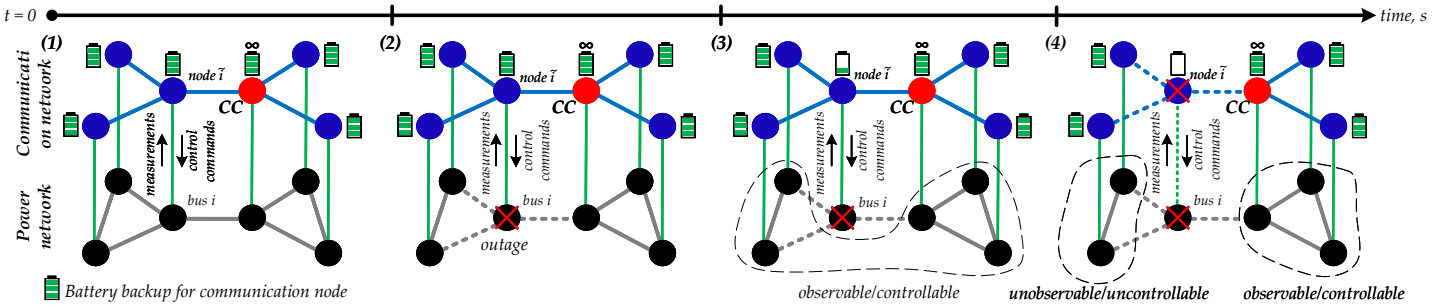

Figure 1: Interdependency across different layers of a representative coupled power-communication system. States (1) to (4) indicate snapshots as time progresses. (1) Pre-outage system. (2) Outage of Bus i leading to the formation of two separate islands within the power network. (3) Battery backup at communication node $\tilde{i}$ preserves the communication node's functionality. Consequently, the power system maintains full observability and controllability. (4) Battery depletion at node $\tilde{i}$ in the communication network results in disconnection of node $\tilde{i}$. As a consequence, one of the islands in the physical layer experiences a loss of observability and controllability.

of the substations in that aggregation has lost power supply from the grid and are using battery backup. Taking this into consideration, we propose the battery backup depletion time to be a function of the ratio $\frac{P_{Load}}{P^0_{Load}}$, where P_{Load} represents the current active load at the bus and P^0_{Load} represents the pre-disturbance active load. The node fails once the battery is fully discharged.

Followings are different possible categories of a node in V_c considering its collocated bus in V_p where P_{Load} and P_{Gen} represent active power load and generation, respectively, in the bus in V_p.

- *Type (1)–$P_{Load} \neq 0$, and $P_{Gen} = 0$:* For nodes collocated with this type of buses, we propose a battery decay characteristic as follows.

$$T_{bat} = c_1 + c_2 tanh\left(c_3 \frac{P_{Load}}{P^0_{Load}}\right); \quad \frac{P_{Load}}{P^0_{Load}} \in [0, c_4] \qquad (4)$$

  where, T_{bat} represents the discharge time of the battery. In (4), c_1 denotes the duration for which the battery backup of a node will sustain its operation in the event of an immediate trip of the collocated bus. To achieve the desired behavior for the battery discharge time, we have selected a function that is concave in $\frac{P_{Load}}{P^0_{Load}}$. As an example, a 'hyperbolic tangent' function has been chosen. The model however is not restricted to this function and one may choose a different function to reflect different specifications and conservativeness of their battery decay model. The values of c_2 and c_3 can be chosen to ensure a desired progressively decreasing slope for T_{bat}. Parameter c_4 determines the threshold above which none of the substations in the corresponding bus are assumed to have lost power supply from the grid, i.e., if the ratio P_{Load}/P^0_{Load} exceeds c_4, the battery for the communication node will not undergo decay. In this paper, we use $c_1 = 10$, $c_2 = 150$, $c_3 = 2.5$, and $c_4 = 0.98$. The corresponding characteristic for T_{bat} is shown in Fig. 2. Since the values of these user-defined constants depend on the system specifications, researchers can determine them according to their needs.
- *Type (2)–$P^0_{Load} = 0$, and $P_{Gen} = 0$:* For this type of node we use $T_{bat} = c_1$ as the battery support discharge time.
- *Type (3)–$P_{Gen} \neq 0$:* The battery backup in node will never fail, unless the generator trips. If generator is tripped in such bus, it will be treated as Type (1) or Type (2).
- *Type (4)–CC:* We assume that battery backup for CC will never discharge (i.e., $T_{bat} = \infty$).

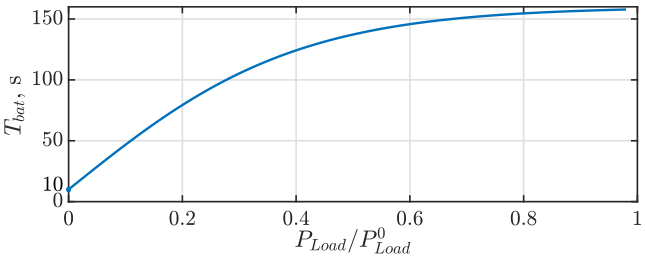

Figure 2: Battery support discharge time for node as a function of the loading level in the collocated load bus.

Remark on battery model:
The model becomes progressively more conservative as we move from a concave to a convex characteristic, indicating a reduction of battery energy storage capacity. For example, a convex characteristic implies even a small fraction of loss of load will lead to a shorter battery support discharge duration compared to Fig. 2. In practice, substations are equipped with reasonable battery backups and therefore a concave function, although less conservative, is more realistic.

C. Modeling of Interdependency

We propose a deterministic cascading failure model for power grids wherein certain interdependencies between the physical and the cyber layer are considered, see Fig. 1. Simulations of our dynamic model make it possible to update the topologies of G_p and G_c and their interconnections with high resolution due to explicit representation of time.

- *Communication link – power line direct interdependency:* The failure of a power line does not immediately lead to the failure of the corresponding communication link (if exists) and *vice-versa.* This is because the communication links are assumed to be based on fiber-optic and/or microwave technology.
- *Node – bus direct interdependency:* If a bus fails first, the collocated node fails after c_1 s. If a node fails first, it does not lead to a bus failure.
- *Active power load – node direct interdependency:* A loss of active power load at a bus leads to a delayed node failure

following (4). There is no direct interdependency between a node outage and the active load at the collocated bus.

Indirect interdependencies: There are multiple indirect interdependencies possible across bus, power line, node, and communication link failures. A communication link/node failure may lead to loss of controllability/observability of an island and as a result may stop application of OPC. This can lead to line overloading and tripping and UVLS. Line trippings can lead bus outage and have a direct impact on node outage. UVLS can also lead to a delayed node outage.

III. Centralized Optimal Preventive Control for Cascading Failure Mitigation

A. OPC Problem

Figure 3 shows the structure of the proposed OPC within CC for cascade mitigation. The averaged values of active power generations and those of nodal voltage magnitudes at generator buses are used as inputs to the OPC to avoid the effect of oscillations stemming from system dynamics. These averaged values are determined from the most recent window of length T^w_{OPC} s preceding the initiation of computations in the OPC. The choice of T^w_{OPC} depends on the most observable low frequency oscillations in the system. In a power grid, electromechanical oscillations (also called 'modes') of multiple frequencies can be observed typically in the range of $0.1-2$ Hz. However, not every oscillation frequency exhibits itself with a high amplitude in measured signals. Higher the observability of the mode, higher the amplitude. Therefore, one needs to consider the window length T^w_{OPC} such that it is close to an integral multiple of the time-period of the signal depending on the highly observable modes. In this paper a fixed T^w_{OPC} is used. This however can be adaptively changed based on knowledge of evolving modal frequencies obtained from the wide-area measurement systems. Additionally, the latest known real and reactive loads, as well as the admittance matrix of the island, are considered as inputs to the optimization problem. We solve this problem exclusively for fully-observable islands to avoid erroneous results that may arise from inaccurate knowledge of the admittance matrix in partially observable islands. Therefore, standard methods for determining observability as routinely done in state estimation [16] are used before solving the optimization problem.

The aims of the optimization problem are to minimize branch overload and load shedding. Due to the potential infeasibility of the optimization problem when using hard constraints for line heating limits, soft constraints are used instead. Subsequently, the user-defined overload variable, $\mathbf{I_{Over}}$, is incorporated into the objective function with a weight of $\boldsymbol{\lambda}$. The OPC problem is formulated as:

$$\underset{\mathbf{P_{Gen}},\mathbf{P_{Load}},\mathbf{Q_{Load}},\mathbf{v_{Gen}}}{\text{minimize}} \quad -\mathbf{1^T P_{Load}} + \boldsymbol{\lambda}^{\mathbf{T}}\mathbf{I_{Over}} \tag{5}$$

subject to:

$$|\mathbf{I_{Line}}| \leq \mathbf{I_{max}} + \mathbf{I_{Over}}, \quad \mathbf{I_{Over}} \geq 0 \tag{6}$$

$$P^{pre}_{i,Load} Q_{i,Load} = P_{i,Load} Q^{pre}_{i,Load}, \ \forall i \in \text{load buses} \tag{7}$$

$$\mathbf{P_{Gen}} - \mathbf{P_{Load}} - \mathbf{P}(\mathbf{v},\theta) = 0 \tag{8}$$

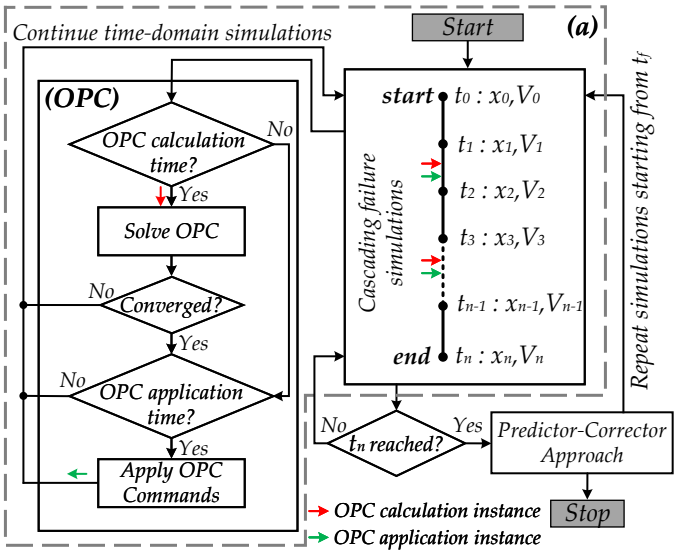

Figure 3: Flowchart of BEM with Predictor-Corrector (BEM-PC) approach for cyber-physical systems with optimal preventive controller (OPC). $t = t_i, i \in \{0, 1, ..., n-1\}$: instants of tiers of cascade. t_f shows earliest instance of oscillatory instability (if there exists any). Trapezoidal method (TM) only applies to the subprocess (a).

$$\mathbf{Q_{Gen}} - \mathbf{Q_{Load}} - \mathbf{Q}(\mathbf{v},\theta) = 0 \tag{9}$$

$$P_i(v,\theta) = \sum_{k=1}^{n_b} v_i v_k (G_{ik} cos\theta_{ik} + B_{ik} sin\theta_{ik}), \forall i \tag{10}$$

$$Q_i(v,\theta) = \sum_{k=1}^{n_b} v_i v_k (G_{ik} sin\theta_{ik} - B_{ik} cos\theta_{ik}), \forall i \tag{11}$$

$$v^{min} \leq v_i \leq v^{max}, \ \forall i \tag{12}$$

$$\mathbf{0} \leq \mathbf{P_{Load}} \leq \mathbf{P^{pre}_{Load}} \tag{13}$$

$$\mathbf{P^{min}_{Gen}} \leq \mathbf{P_{Gen}} \leq \mathbf{P^{pre}_{Gen}} \tag{14}$$

$$\mathbf{Q^{min}_{Gen}} \leq \mathbf{Q_{Gen}} \leq \mathbf{Q^{max}_{Gen}} \tag{15}$$

where, vectors are denoted in bold letters; $|\mathbf{I_{Line}}|$ indicates the vector of absolute values of elements of $\mathbf{I_{Line}} \in \mathbb{C}^p$; $\mathbf{I_{Line}}$ and $\mathbf{I^{max}}$ show vectors of line currents and maximum allowable current flows in lines, respectively; $\mathbf{I_{Over}}$ denotes the magnitude of overcurrent of lines; $\mathbf{P_{Load}}$ and $\mathbf{Q_{Load}}$ ($\mathbf{P^{pre}_{Load}}$ and $\mathbf{Q^{pre}_{Load}}$) show vectors of active and reactive loads as decision variables and their input values to the OPC problem, respectively; $\mathbf{P_{Gen}}$ and $\mathbf{Q_{Gen}}$ are vectors of active and reactive power generations; P_i and Q_i denote active and reactive power injections in bus i; $\theta_{ik} = \theta_i - \theta_k$ where θ_i is voltage angle of bus i; G_{ik} and B_{ik} are conductance and susceptance of the line connecting buses i and k; $\mathbf{P^{min}_{Gen}}$ and $\mathbf{P^{pre}_{Gen}}$ are vectors of minimum allowable active power generations and active power generations as inputs to the OPC problem; similarly $\mathbf{Q^{min}_{Gen}}$ and $\mathbf{Q^{max}_{Gen}}$ are vector of minimum and maximum allowable reactive power generations; and finally v^{min} and v^{max} are minimum and maximum allowable voltage magnitudes in buses.

Constraint (6) is included to transform the line flow hard constraint into a soft constraint; (7) maintains a predefined power factor at bus i; (8)-(11) are the active and reactive

power balance constraints at load buses; (12) reflects voltage magnitude of buses should be within the allowable voltage range; (13)-(14) ensures that the OPC solution does not command to increase load and generation while ensuring they don't violate respective minimum values; (15) are constraints for reactive power generation.

In our proposed cascade prevention controller, we leverage the Extended OPF Formulation in MATPOWER [17]. The OPC is a nonlinear programming (NLP) problem that is solved using the *fmincon* routine.

Remark on the choice of parameter $\boldsymbol{\lambda}$:
The parameter $\boldsymbol{\lambda}$ determines a trade-off between the allowable maximum overloading of lines and the load shedding commanded by the OPC. A very large $\boldsymbol{\lambda}$ leads to more 'weight' on the second term of the objective function, and would allow larger load shedding at the cost of small line overloading. This will go against the objective of cascade prevention with minimum load shedding. On the other hand, a very small $\boldsymbol{\lambda}$ results in negligible load shedding while allowing a higher line overloading, which will reduce the effectiveness of OPC. Therefore, a balance needs to be developed by appropriately choosing $\boldsymbol{\lambda}$ that will depend on the system under consideration. In our case, $\boldsymbol{\lambda} = 100 \times \mathbf{1}$ ($\mathbf{1}$ shows all-ones vector) gave an acceptable tradeoff following an educated trial and error under the above guideline.

B. Time-Synchronized Application of OPC Commands for Cascade Mitigation

Following convergence, let the optimal values of the decision variables be $(\mathbf{P}^*_{\mathbf{Gen}}, \mathbf{P}^*_{\mathbf{Load}}, \mathbf{Q}^*_{\mathbf{Load}}, \mathbf{v}^*_{\mathbf{Gen}})$, which are desired setpoints (also called OPC commands) for active power generations, active and reactive loads, and voltage magnitudes in PV buses, respectively. We limit the application of OPC commands to fully-controllable islands that have complete access to the actuators (generators and load buses with nonzero loads) within the island. This requirement is essential because partial application of OPC commands within an island is likely to deteriorate its effectiveness.

In this paper, an observable/controllable island is defined as one where every bus within the island possesses an operational collocated communication node, establishing a connection to CC via a network of communication links. Under the realistic assumption that each communication node is equipped with a backup battery, in cases where one or more buses within the island experience failures, the co-located communication nodes can be relied upon to transmit data packets to the CC. This data transfer process ensures the CC receives accurate information regarding the resulting sub-island's Y_{bus} configuration, preserving our ability to monitor the island's state. For a visual representation of the interplay between the power and communication systems, please refer to Fig. 1. Therefore, as long as data is received from each node to CC, the island is considered to be controllable. The controllability of an actuator node is determined by the availability of data samples at the latest instant from that node at CC.

Let T^{Time}_{OPC} indicate the CPU-time for convergence of the optimization problem in CC. Note that the dynamic simulation of the cascading failure of the cyber-physical model runs in parallel and as presented in Fig. 3, the desired setpoints are communicated to the actuators in the model after T^{Time}_{OPC} s following the initiation of computations in OPC. Note that this time synchronization with the dynamic simulation is important to emulate realistic preventive control actions.

The $\mathbf{P}^*_{\mathbf{Gen}}$ commands are used as setpoints of mechanical power inputs of generators. The $\mathbf{P}^*_{\mathbf{Load}}$ and $\mathbf{Q}^*_{\mathbf{Load}}$ commands are sent to respective load buses to perform load shedding. The $\mathbf{v}^*_{\mathbf{Gen}}$ commands are sent to generator excitation systems augmented by a proposed integral-controller – see Fig. 15 in Appendix. As shown in Fig. 15, the integral control makes the voltage reference tracking possible. We have shown in our case studies that the performance of OPC deteriorates without voltage tracking.

Remarks on OPC:
1. As described in the Introduction section, the state-of-art in OPC for cascade prevention is based on DC power flow, which assumes a 'flat' voltage provide and does not consider reactive power. On the other hand, our approach is based on AC power flow, which does not have such limitations and can accommodate constraints (7), (9), (12), and (15). In addition, the proposed integral control action in excitation systems is new in our method. Therefore, the effectiveness and competitiveness of state-of-art OPC is fundamentally limited compared to our approach.
2. The objectives of our proposed OPC and the security-constrained optimal power flow (SCOPF) [18] differ from each other. SCOPF determines generator dispatch in absence of any load shedding with the objective of minimizing generation cost subject to security constraints. In contrast, OPC determines generator dispatch and their terminal voltages with the objective of minimizing overloading in lines and load shedding, subject to multiple constraints.

Remark on use of SCADA:
This paper assumes WAMPAC network as part of the cyber layer, where PMUs are assumed to be installed in all buses of the system. We acknowledge that our research focuses on a futuristic power grid, since today's power system is dominated by SCADA. For using SCADA systems for OPC proposed in this paper, sampling rate should be higher, say at least 1 Hz. This will allow a bare minimum number of samples in the window of size $T^w_{OPC} = 5$ s used in the paper. Even in that case, the OPC performance is expected to be worse compared to that from WAMPAC. To improve the performance of SCADA-based OPC, new approaches might be needed. Therefore, the analysis with SCADA is outside the scope of this work, and will be considered in a future paper.

IV. Time-Domain Simulation Process

At the outset, we recommend that readers refer to [3] for details of dynamic simulations of cascading failures, particularly the BEM-PC approach. The time-domain simulations for cascading failures involve the formation and independent solution of Initial Value Problems (IVPs) on sets of DAEs (1)-(3). An event refers to any discontinuity that arises from a discrete change in the system, such as a relay action resulting in a change in the values of the z vector. Two approaches exist for solving IVPs in power systems - partitioned and simultaneous

[14], [19]. For this purpose, we use the simultaneous approach with implicit integration method, which is more efficient for simulations with variable time-step.

In the dynamic simulation of cascading failures in complex power grids with coupled cyber and physical layers, it may not be necessary to capture detailed transient oscillatory behavior of the system, as long as: (i) the model can accurately capture the cascade propagation path and end results as in ground truth, and (ii) the model is suitable for statistical analysis. In this context, using large time steps would be desirable to speed up the simulation. However, the integration method must be robust enough to handle large time steps and avoid divergence, while producing accurate end results. To this end, we apply our newly-proposed BEM-PC [3] to solve the IVPs. Results in [3] indicate that BEM-PC is suitable for statistical analysis and can replicate end results as in Trapezoidal method (TM) with high accuracy. In this paper, we refer the results obtained by TM as '*ground truth*'.

A. Simulation Approach

The flowchart in Fig. 3 illustrates the simulation approach utilizing BEM-PC for conducting cascading failure simulations in cyber-physical power systems. The approach includes OPC to optimize cascade mitigation. Although the proposed model is parallelizable, for the purposes of this paper, all simulations were implemented serially.

Subprocess (a) – Cascading failures simulation and optimal preventive control: This subprocess involves conducting cascade simulations using variable time-step BEM with a stiff decay property [20] that enables the use of large steps to accelerate dynamic simulations by disregarding fast oscillations in the exact time-domain trajectories. The cascading failure is triggered by inducing initial node outages and tripping of connected lines to those buses in the power network at time t_0. Following each event, IVP(s) are solved with a known initial condition (x_0, V_0, z_0) for each island. The appropriate relays are modeled in the cascade simulations, resulting in a series of events during severe contingencies such as line tripping, out-of-step machine tripping, and load shedding.

During the time-domain simulations, the optimal control time $t = kT_C$ is repeatedly checked, where T_C is a predetermined fixed interval between two consecutive instants of initiating OPC calculations and k is an integer. In other words, the optimal control time is the time instant for initiating OPC calculations. If it is reached, the OPC is calculated using (5)-(15), as described in III. The OPC is conducted only on fully observable islands every T_C s. The value of T_C should be chosen based on a multitude of factors like the typical convergence time of OPC, generation ramp rates, and effectiveness of OPC among others. For example, the first two factors will restrict the minimum value of T_C while the third factor will determine it's maximum value. Therefore, system planners should determine this value based on offline studies. In addition, subprocess (a) repeatedly checks if the appropriate time to apply OPC commands has been reached for those islands with converged OPC, and then the appropriate commands are communicated to the power network's actuators. Simulations in subprocess (a) are terminated if (i) steady-state is attained in the time-domain simulation, and no anticipated relay action or pending application of OPC is observed, or (ii) an island blackout is detected.

Predictor-Corrector Approach: This subprocess addresses the hyperstability issue of BEM. More particular, BEM converges to the unstable equilibrium of the system in presence of oscillatory instability, which leads to a stable simulation result. The predictor identifies oscillatory instability based on eigendecomposition of the system matrix at the post-disturbance unstable equilibrium obtained as a byproduct of BEM. The corrector uses right eigenvectors to identify the group of machines participating in the unstable mode. This helps in applying appropriate protection schemes as in ground truth. Since BEM-PC is not the main focus of this work, we refer the readers to our paper [3] to avoid repetition.

B. Some Important Aspects of Implementation

In this section, we present some important aspects regarding the implementation of both TM and BEM-PC methods. For both methods we utilize: (i) full Newton's method, (ii) analytical Jacobian matrix calculation during Newton iterations, (iii) sparse calculations/data storage, (iv) Matlab's most comprehensive inversion routine for Jacobian inversion in time-domain simulations, as depicted in the flowchart in [21], (v) variable time step integration, (vi) an adaptive center-of-inertia (COI) reference frame proposed in [3] for the efficient convergence of Newton iterations, and finally (vii) identical methods for OPC (presented in section III).

Some other important aspects include:

1. *Variable step-size in integration:* To improve the speed of the time-domain simulations, we utilize adaptive time step-size control based on local truncation error (LTE) [22] for TM and a separate strategy for BEM-PC, see [3]. The variable time approach allowed for larger time steps when the solution was not varying rapidly, leading to a more efficient simulation process.
2. *Stopping criteria:* We incorporated the following stopping criteria in our simulations for an island: i) the speed variations of machines in a predetermined window length falls below a certain threshold and no future relay actions and application of OPC commands are expected, or ii) a complete collapse is observed.
3. *Software platform:* We constructed the proposed model from the first principles in Matlab [23]. For initialization of time-domain simulations, we utilized MATPOWER [17] for power flow solutions.

V. Case Studies

In this section, the simulation results of proposed dynamic model, as well as the effectiveness of the proposed cascade mitigation approach in interdependent cyber-physical power systems, are illustrated using the IEEE 118-bus system and the Polish network during the winter peak of 1999-2000 [17]. Two types of numerical integration methods (traditional TM and newly proposed BEM-PC [3]) are used in the dynamic simulations of the proposed model and a comparison of the results are presented.

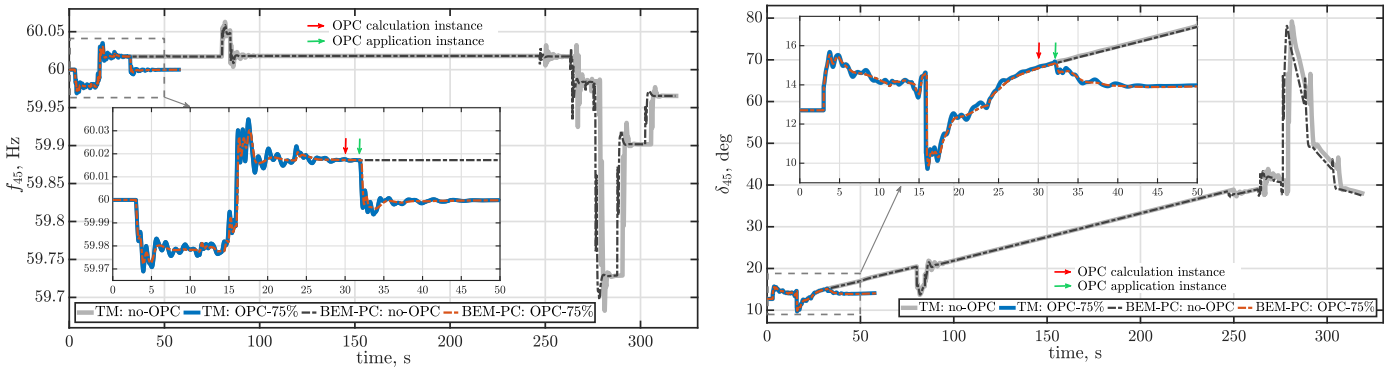

Figure 4: BEM-PC vs TM with OPC-75% vs without OPC results for a case in IEEE 118-bus test system – time-domain plots of machine speed (f) and rotor angle (δ) for $G45$.

Table I: (a) End of cascade error, (b) path agreement measure, and (c) run time in TM w.r.t. BEM-PC: IEEE 118-Bus System

		No-OPC				OPC–MST			
		mean	min	max	median	mean	min	max	median
error in state of	buses	0.982	0	48	0	1.127	0	86	0
	machines	0.454	0	24	0	0.522	0	38	0
	lines	1.462	0	73	0	1.801	0	128	0
maximum error in	$\|v\|, pu$	0.009	0	0.090	0.003	0.015	0	0.190	0.004
	$\angle v, deg.$	1.509	0	35.390	0.065	1.588	0	34.735	0.111
	f, Hz	0.127	0	5.933	8.1e-5	0.130	0	8.553	1e-4
R		0.957	0	1	1	0.937	0	1	1
runtime ratio		9.041	0.191	74.584	8.763	10.267	0.146	74.004	9.140
		OPC–75%				OPC–ideal			
		mean	min	max	median	mean	min	max	median
error in state of	buses	1.147	0	90	0	1.145	0	105	0
	machines	0.541	0	38	0	0.532	0	47	0
	lines	1.876	0	128	0	1.820	0	153	0
maximum error in	$\|v\|, pu$	0.019	0	0.182	0.008	0.021	0	0.153	0.010
	$\angle v, deg.$	1.429	0	30.270	0.177	1.394	0	29.176	0.191
	f, Hz	0.058	0	6.178	2e-4	0.057	0	5.251	2e-4
R		0.933	0	1	1	0.923	0	1	1
runtime ratio		12.565	0.156	159.301	10.596	12.917	0.175	64.645	11.938

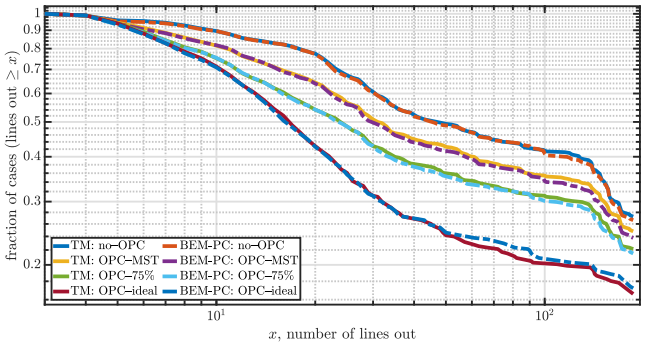

Figure 5: Fraction of cases with line outage $\geq x$ at the end of cascade: IEEE 118-bus system.

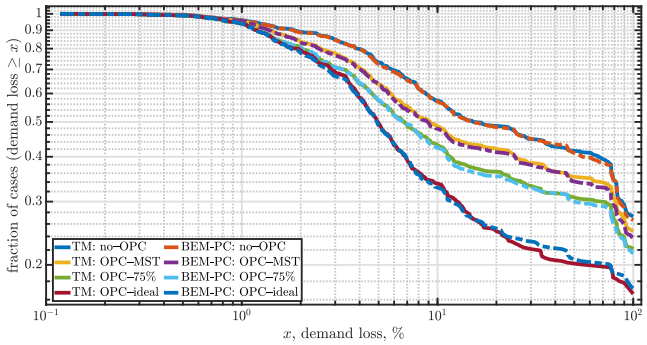

Figure 6: Fraction of cases with % demand loss $\geq x$ at the end of cascade: IEEE 118-bus system.

Table II: Improvement in end of cascade average demand loss (%) and number of line outages through proposed OPC in TM and BEM-PC w.r.t. no-OPC model: IEEE 118-bus system

Improvement in		MST	75%	Ideal
Demand loss %	TM	5.681	10.166	19.421
	BEM-PC	6.133	10.354	18.478
Line outage	TM	11.143	20.331	37.604
	BEM-PC	11.967	20.598	35.819

The IEEE 118-bus system consists of 118 buses, 54 machines, and 186 branches, while the Polish system is a large-scale network with 2,383 buses, 327 machines, and 2,896 lines. Synthetic dynamic data are generated for both models. Cascades are triggered with 2 and 3 initial node outages, respectively, for the IEEE 118-bus and Polish systems. These initial outages are sufficient to create long-term cascading sequences in these networks. Relay characteristics and other

physical layer modeling parameters are used as in [3].

We consider the following scenarios: (i) a no-OPC scenario, in which the optimal preventive controller is deactivated; (ii) an OPC-ideal scenario, which assumes that communication nodes never fail due to infinite battery backup; (iii) an OPC-MST scenario, which employs Topology (1); and (iv) an OPC-$q\%$ redundancy scenario, which employs Topology (2) with $q = 100\beta$.

For OPC, we utilized $\boldsymbol{\lambda} = 100\times\mathbf{1}$ ($\mathbf{1}$ shows all-ones vector), $T_C = 30$ s, and $T^w_{OPC} = 5$ s. To determine T^{Time}_{OPC} for the IEEE 118-bus system, we use the actual CPU-time of the optimization algorithm employed in OPC. However, for the Polish system the actual CPU-time is too long due to a limited computational power at our end. We consider a dedicated and powerful computer hardware in CC that can achieve $T^{Time}_{OPC} = 1$ s for all converged cases of OPC. We perform Monte-Carlo simulations with 500 random initial node outages across five servers with a 2.2 GHz Intel Xeon Processor, 20 CPUs per server, and 128 GB of RAM in PSU's ROAR Collab facility [24]. The TM based dynamic simulation is assumed to reflect the ground truth and is used as the benchmark.

A. IEEE 118-bus system

Figure 4 depicts time-domain simulations of rotor angle and speed of machine $G45$ for a generic case in the IEEE 118-bus system. The simulations compare the results of BEM-PC with and without OPC against TM with and without OPC. In cases with OPC, we employed a communication network that has a 75% degree of redundancy with the power system. The results show that BEM-PC and TM with OPC were able to serve $\sim 79\%$ of the demand at the end of the cascade, while BEM-PC and TM without OPC served only $\sim 59\%$ of the demand. This indicates that the proposed OPC approach was effective and confirms the ability of BEM-PC in tracking TM. Furthermore, BEM-PC with OPC is ~ 16 times faster than TM with OPC, while BEM-PC without OPC is ~ 10 times faster than TM without OPC, confirming the efficiency of BEM-PC. The last two observations are not shown in Fig. 4.

Figures 5 and 6 illustrate the frequency of occurrence of the number of line outages and demand loss at the end of a cascade exceeding a certain level in various scenarios for coupled power-communication network simulations using TM and BEM-PC. The results demonstrate the effectiveness of the proposed cascade mitigation approach described in section III. The OPC-ideal scenario significantly reduces demand loss and the number of line outages at the end of a cascade. Additionally, even OPC-75% and OPC-MST, which employ less conservative topologies of the WAMPAC network, can effectively mitigate the propagation of cascades in the IEEE 118-bus test system. Furthermore, the results of TM and BEM-PC are consistent across all scenarios, as shown in Figs 5 and 6. Some minor disparity can be observed between BEM and TM for very large number of line outages and demand loss, especially for OPC-ideal cases.

Based on 500 Monte-Carlo simulations, Table I presents a comprehensive comparison of the accuracy of BEM-PC w.r.t. TM in terms of errors in the status (connected or disconnected) of buses, machines, and lines at the end of a cascade event. The table also shows the maximum errors in the voltage magnitude, voltage angles of buses, and system frequency. Despite the presence of some outliers that result in an increase in average error values, BEM-PC is able to replicate the exact end-result of TM for most of contingencies. The path agreement measure (R) [3], [25] compares dependent branch outages (tripped lines after initial disturbance, excluding initial disconnections to trigger the cascade) in the corresponding contingencies in TM and BEM-PC where value of $R = 1$ indicates complete agreement in dependent line outages and path of cascade in two approaches. Different measures for R in Table I show that the models have almost complete agreement in the cascade path. Generally, as we move from the no-OPC scenario to the OPC-ideal scenario, errors tend to increase. Finally, the runtime ratio measures in the table indicate that BEM-PC is, on average, $\approx 9-13$ times faster than TM.

Table III: Improvement in end of cascade average demand loss ($\%$) and number of line outages through proposed OPC in TM and BEM-PC w.r.t. no-OPC model: IEEE 118-bus system - without integral-controller

Improvement in		MST	75%	Ideal
Demand loss $\%$	TM	0.666	2.579	10.442
	BEM-PC	-1.181	1.122	9.666
Line outage	TM	1.245	5.197	20.390
	BEM-PC	-1.906	2.816	18.956

The results in Table II underscore the effectiveness of the proposed OPC in mitigating cascading events, as evidenced by the significant improvement in both demand loss and the number of line outages. These values represent the average of differences between end-of-cascade demand loss ($\%$) and number of line outages in scenarios with OPC w.r.t. no-OPC obtained from the exhaustive simulations. Moreover, a comparative analysis of BEM-PC and TM approaches shows that they yield similar end results, further validating the accuracy of proposed BEM-PC approach for dynamic simulations of coupled power-communication networks. Finally, Table III presents similar results to those in Table II for the proposed models without integral controllers designed for the application of OPC commands. This table highlights the importance of including integral controllers in the models.

B. Polish system

We conducted simulations for the coupled power-communication network using the IEEE $2,383$-bus Polish system to observe the impact of our proposed OPC described in section III. To this end, we compare the accuracy of BEM-PC w.r.t. TM based on 500 Monte-Carlo simulations for different scenarios including no-OPC, OPC-MST, OPC-85%, and OPC-ideal. The results are presented in Figs 7 and 8, which respectively show the frequency of occurrence of the number of line outages and demand loss at the end of a cascade exceeding a certain level x. The results highlight the importance of redundancy in the cyber layer and demonstrate the effectiveness of the proposed cascade mitigation approach. The OPC-ideal scenario, which employs an ideal WAMPAC network, is shown to significantly reduce demand loss and the number of line outages at the end of a cascade w.r.t. no-OPC case. It is worth noting that the effectiveness of OPC

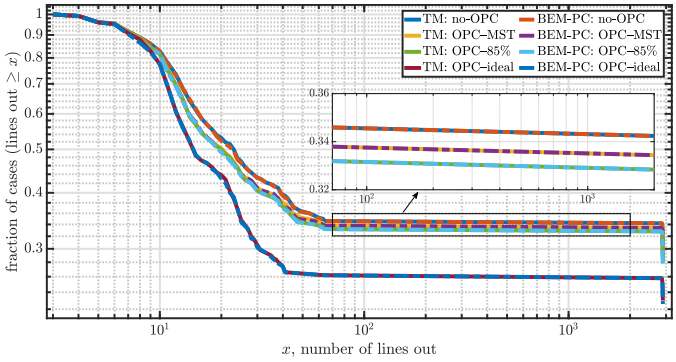

Figure 7: Fraction of cases with line outage $\geq x$ at the end of cascade: Polish system.

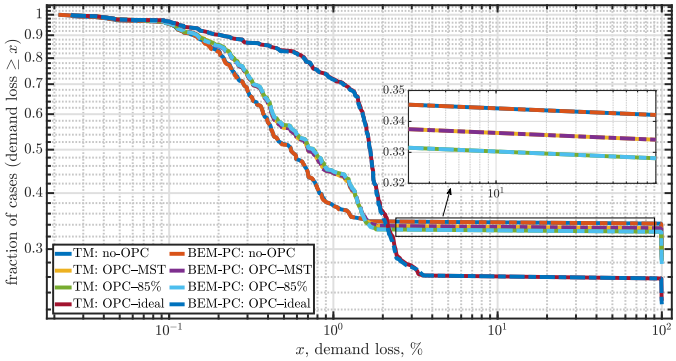

Figure 8: Fraction of cases with % demand loss $\geq x$ at the end of cascade: Polish system.

is visible for contingencies resulting in demand losses higher than 2%, as shown in Fig. 8. However, when $x = 1 - 2\%$ range is considered in Fig. 8, we observe a counter-intuitive trend. This can be attributed to the impact of load shedding commanded by OPC, which does not take place in the no-OPC scenario. Furthermore, this phenomenon is more pronounced in the OPC-ideal case compared to OPC-MST and OPC-85%. This can be explained by the presence of a higher number of fully observable and controllable islands in the OPC-ideal scenario. Nevertheless, Fig. 7 illustrates that the proposed OPC exhibits consistent effectiveness in reducing line outages for all cases. Furthermore, the results of TM and BEM-PC are consistent across all scenarios, as shown in Figs. 7 and 8.

Table IV compares various error measures at the end of cascade for BEM-PC w.r.t. TM for various scenarios. These indicate that for almost all of the cases, BEM-PC is able to accurately mimic the end results of cascade as in TM. The R measures in this table demonstrate that the models have a high degree of agreement in the cascade path. Finally, the runtime ratio indicates that on average BEM-PC is $\approx 22 - 26$ times faster than TM. Finally, the effectiveness of the proposed OPC in mitigating cascading events is underscored by the results presented in Table V, which reveal a considerable improvement in the number of line outages.

Remarks on BEM-PC:

1. In this work, we have generated significantly more severe cascading failure events compared to [3] to demonstrate the effectiveness of the proposed OPC approach. This has been achieved by reducing the line current ratings by 10% in IEEE 118-bus system and 5% in the Polish system compared to [3]. This is a probable cause for a slightly lower accuracy observed in the BEM-PC results w.r.t. TM, as compared to the findings presented in [3].

2. We skip the presentation of BEM-PC performance results in cases of oscillatory instability in this paper, as these have already been comprehensively studied in [3].

Remark on interdependent cyber-physical systems: For Polish system in Figs 7 and 8, the OPC-ideal scenario shows significant improvement in line outage and demand loss at the end of cascade w.r.t. the no-OPC scenario. In contrast, the non-ideal OPC scenarios show limited improvement compared to the scenarios without preventive control. This signifies the importance of considering realistic interdependent cyber and physical layers in the cascading failure model.

C. Effect of latency and time skew

As described at the beginning of Section II-B1, we are assuming the WAMPAC is available for the entire system. Let us focus on the following facts regarding time skew and latency in WAMPAC networks.

1. Time skew from clock drift error: PMUs measure voltages and currents and output measured data at typically 60 samples/s. Each sample is time-stamped through a global positioning system (GPS) clock with microsecond precision. So, any clock drift error and related time-skew would be negligible.

2. Data communication and latency buildup: The time-stamped measurements are then communicated to local phasor data concentrators (PDCs), which then communicate the data to regional PDCs (also called super PDCs). There could be another hierarchy of super PDCs, which finally send the data to CC where the central PDC will process the data. In the process of sending data packets from multiple PMUs, the latency varies in a stochastic manner. It also depends on factors like congestion. Therefore, when data from individual PMUs arrive at the PDC location, the data packets with the same time stamp do not arrive at the same time. The PDC waits for all samples with the same time stamp to arrive. It then 'synchronizes' them and sends it forward. Unfortunately, PDCs contribute a lot to the delay as well.

3. Typical latency studied for closed-loop control application: Latencies of the order of hundreds of milliseconds have been studied in literature on near real-time control applications of WAMPAC, see for example [26]–[30]. In line with the literature in this area, we have considered a 500 ms maximum end-to-end latency in our study.

4. Modeling the impact of latency and time skew: As described earlier, typical time skew is of the order of microseconds, which is negligible compared to the inter-sample interval of $1/60$ s. Therefore, this will not cause error during the time-synchronization of samples at the PDC in CC. Since the effect of time skew is negligible, following this synchronization, a 500 ms maximum end-to-end latency of each batch of samples from all PMUs can be modeled by time-shifting the moving

Table IV: (a) End of cascade error, (b) path agreement measure, and (c) run time in TM w.r.t. BEM-PC: Polish System

		No-OPC				OPC–MST			
		mean	min	max	median	mean	min	max	median
error in	buses	0.143	0	16	0	0.218	0	23	0
state of	machines	0.189	0	4	0	0.143	0	4	0
	lines	0.157	0	15	0	0.297	0	30	0
maximum	$\|v\|, pu$	0.001	0	0.043	1e-4	0.001	0	0.125	1e-4
error in	$\angle v, deg.$	0.129	0	15.407	0.002	0.200	0	22.864	0.003
	f, Hz	0.013	0	0.300	4e-5	0.011	0	0.300	4e-5
R		0.991	0.666	1	1	0.974	0.464	1	1
runtime ratio		26.045	0.627	74.512	24.348	22.845	0.645	79.092	21.646
		OPC–85%				OPC–ideal			
		mean	min	max	median	mean	min	max	median
error in	buses	0.143	0	16	0	0.096	0	6	0
state of	machines	0.132	0	4	0	0.046	0	2	0
	lines	0.197	0	15	0	0.197	0	12	0
maximum	$\|v\|, pu$	1.6e-3	0	0.078	2e-4	0.004	0	0.150	3e-4
error in	$\angle v, deg.$	0.121	0	15.407	3.4e-3	0.142	0	6.751	0.014
	f, Hz	0.012	0	0.328	5e-5	0.007	0	0.328	3e-5
R		0.977	0.5	1	1	0.974	0.5	1	1
runtime ratio		22.310	0.579	72.710	21.948	24.711	0.619	71.526	25.122

Table V: Improvement in end of cascade average demand loss (%) and number of line outages through proposed OPC in TM and BEM-PC w.r.t. no-OPC model: Polish system

Improvement in		MST	85%	Ideal
Demand	TM	0.712	1.297	7.713
loss %	BEM-PC	0.710	1.297	7.721
Line	TM	23.766	41.140	243.716
outage	BEM-PC	23.834	41.164	243.772

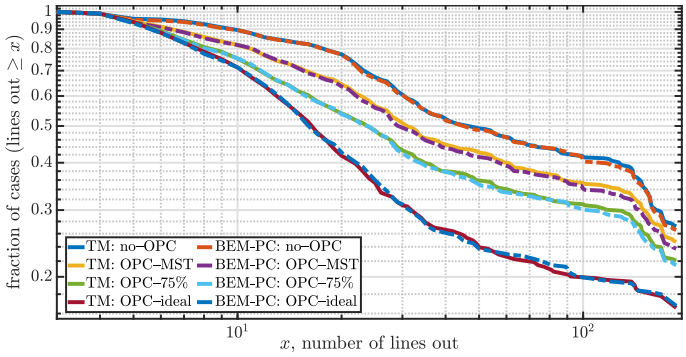

Figure 9: Latency of 500 ms is considered for OPC data input. Fraction of cases with line outage $\geq x$ at the end of cascade in IEEE 118-bus system.

window of data used in OPC by 0.5 s in the past while retaining the window size.

We have studied the impact of latency on OPC performance in IEEE 118-bus system. Figures 9 and 12 show the frequency of occurrence of the number of line outages and demand loss at the end of a cascade exceeding a certain level for TM and BEM-PC. A qualitative comparison of these results with those in Figs 5 and 6 indicate that the impact of the latency is barely noticeable.

Boxplots in Figs 10 and 11 show the central tendency of the differences in line outages between the cases with 0.5 s delay and no delay for TM and BEM-PC, respectively. It can be seen that the median difference is zero and only a few outliers are observed. This observation is similar in the context of % demand loss comparison shown in Figs 13 and 14.

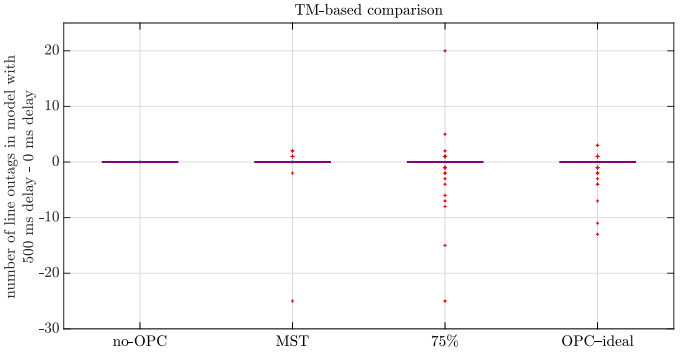

Figure 10: For TM: Boxplots of the difference in line outages at the end of cascade in IEEE 118-bus system between 500 ms delay and 0 ms delay.

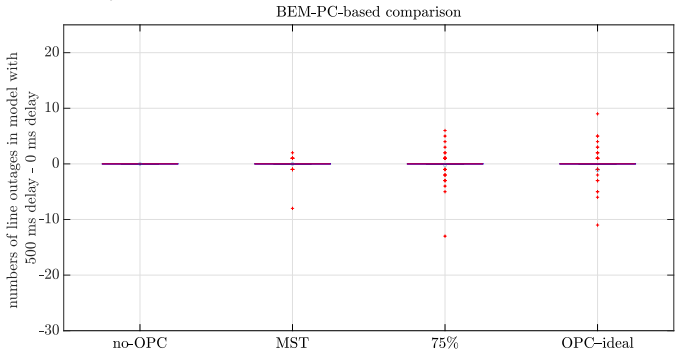

Figure 11: For BEM-PC: Boxplots of the difference in line outages at the end of cascade in IEEE 118-bus system between 500 ms delay and 0 ms delay.

VI. Conclusion and Future Work

This paper presented a dynamic cascading failure model that considers realistic interdependencies in power grids with physical and cyber layers. The model considered delay in disconnection of communication nodes following bus outages and load sheddings due to the depletion of battery backup in those nodes. The proposed centralized OPC was most effective

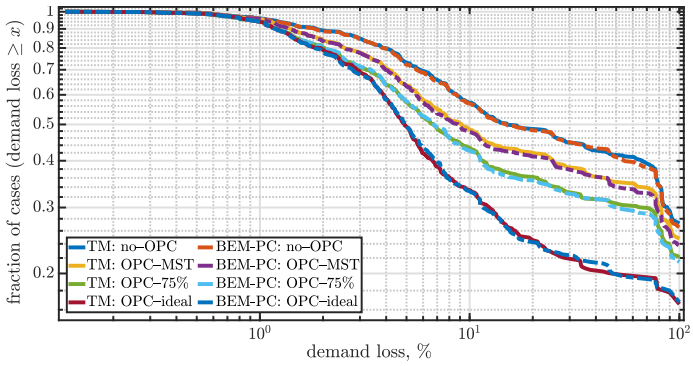

Figure 12: Latency of 500 ms is considered for OPC data input. Fraction of cases with % demand loss $\geq x$ at the end of cascade in IEEE 118-bus system.

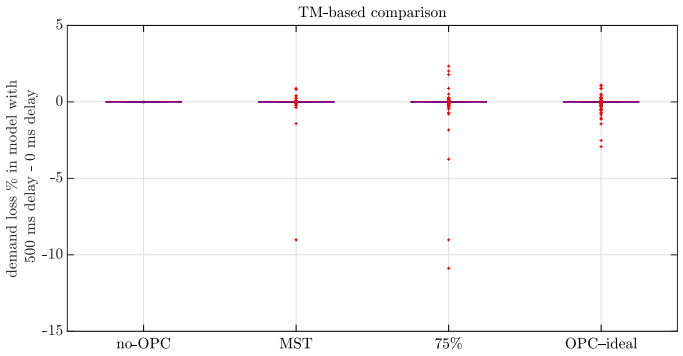

Figure 13: For TM: Boxplots of the difference in % demand loss at the end of cascade in IEEE 118-bus system between 500 ms delay and 0 ms delay.

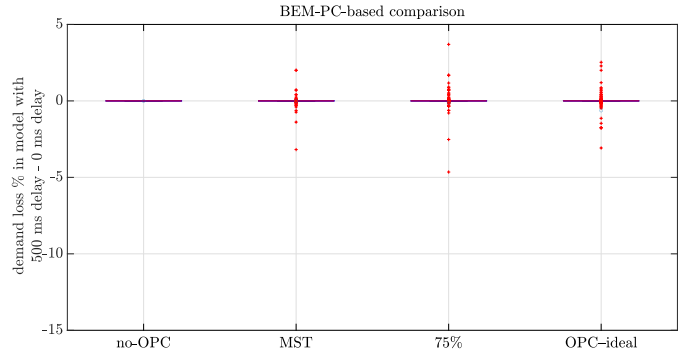

Figure 14: For BEM-PC: Boxplots of the difference in % demand loss at the end of cascade in IEEE 118-bus system between 500 ms delay and 0 ms delay.

in majority of cases under the ideal communication scenario with infinite battery backup while the generator exciters were equipped with voltage tracking integral control. As expected, its effectiveness went down with realistic cases considering finite battery backup. This highlighted the importance of including interdependent cyber and physical layers in a realistic manner. In addition, application of BEM-PC accelerated the Monte-Carlo simulations by a factor of $\approx 9-13$ for IEEE 118-bus system and $\approx 22-26$ for Polish network w.r.t. the TM-based simulations. Future work can focus on extending the proposed approach for including topology estimation problem for the partially observable islands, and applying OPC on the estimated islands. This can lead to the more efficient cascade mitigation approach than it was proposed in this paper.

REFERENCES

[1] P. Henneaux *et al.*, "Benchmarking quasi-steady state cascading outage analysis methodologies", *2018 IEEE Int. Conf. on Prob. Methods Applied to Power Systems (PMAPS)*, pp. 1–6, 2018.

[2] S. Gharebaghi, S. G. Vennelaganti, N. R. Chaudhuri, T. He, and T. F. L. Porta, "Inclusion of pre-existing undervoltage load shedding schemes in ac-qss cascading failure models", *IEEE Transactions on Power Systems*, vol. 36, no. 6, pp. 5645–5656, 2021.

[3] S. Gharebaghi, N. R. Chaudhuri, T. He, and T. La Porta, "An approach for fast cascading failure simulation in dynamic models of power systems", *Applied Energy*, vol. 332, p. 120 534, 2023.

[4] Y. Cai, Y. Li, Y. Cao, W. Li, and X. Zeng, "Modeling and impact analysis of interdependent characteristics on cascading failures in smart grids", *International Journal of Electrical Power & Energy Systems*, vol. 89, pp. 106–114, 2017.

[5] S. G. Vennelaganti, N. R. Chaudhuri, T. He, and T. L. Porta, *Topology estimation following islanding and its impact on preventive control of cascading failure*, 2021. arXiv: 2104.06473 [eess.SY].

[6] Y. Cai, Y. Cao, Y. Li, T. Huang, and B. Zhou, "Cascading failure analysis considering interaction between power grids and communication networks", *IEEE Transactions on Smart Grid*, vol. 7, no. 1, pp. 530–538, 2015.

[7] H. Guo, S. S. Yu, H. H. Iu, T. Fernando, and C. Zheng, "A complex network theory analytical approach to power system cascading failure—from a cyber-physical perspective", *Chaos: An Interdisciplinary Journal of Nonlinear Science*, vol. 29, no. 5, p. 053 111, 2019.

[8] X. Gao, M. Peng, K. T. Chi, and H. Zhang, "A stochastic model of cascading failure dynamics in cyber-physical power systems", *IEEE Systems Journal*, vol. 14, no. 3, pp. 4626–4637, 2020.

[9] X. Gao, M. Peng, and K. T. Chi, "Impact of wind power uncertainty on cascading failure in cyber–physical power systems", *Physica A: Statistical Mechanics and its Applications*, vol. 583, p. 126 358, 2021.

[10] M. Rahnamay-Naeini and M. M. Hayat, "Cascading failures in interdependent infrastructures: An interdependent markov-chain approach", *IEEE Transactions on Smart Grid*, vol. 7, no. 4, pp. 1997–2006, 2016.

[11] V. Farhadi, S. G. Vennelaganti, T. He, N. R. Chaudhuri, and T. La-Porta, "Improvement of scada-based preventive control under budget constraints", *IEEE Transactions on Network Science and Engineering*, vol. 9, no. 4, pp. 2601–2616, 2022.

[12] V. Farhadi, S. G. Vennelaganti, T. He, N. R. Chaudhuri, and T. La Porta, "Budget-constrained reinforcement of scada for cascade mitigation", in *2021 International Conference on Computer Communications and Networks (ICCCN)*, IEEE, 2021, pp. 1–9.

[13] M. Korkali, J. G. Veneman, B. F. Tivnan, J. P. Bagrow, and P. D. Hines, "Reducing cascading failure risk by increasing infrastructure network interdependence", *Scientific reports*, vol. 7, no. 1, p. 44 499, 2017.

[14] P. W. Sauer, M. A. Pai, and J. H. Chow, *Power system dynamics and stability: with synchrophasor measurement and power system toolbox*. John Wiley & Sons, 2021.

[15] S. K. Khaitan and A. Gupta, *High performance computing in power and energy systems*. Springer, 2012.

[16] A. Monticelli, "Electric power system state estimation", *Proceedings of the IEEE*, vol. 88, no. 2, pp. 262–282, 2000.

[17] R. D. Zimmerman *et al.*, "Matpower: Steady-state operations, planning, and analysis tools for power systems research and education", *IEEE Trans.Power Syst.*, vol. 26, no. 1, pp. 12–19, 2011.

[18] A. J. Wood, B. F. Wollenberg, and G. B. Sheblé, *Power generation, operation, and control*. John Wiley & Sons, 2013.

[19] P. Kundur, *Power system stability and control*. NY, USA: McGraw-Hill, 1994.

[20] U. M. Ascher and L. R. Petzold, *Computer methods for ordinary differential equations and differential-algebraic equations*. Siam.

[21] [Online]. Available: https://mathworks.com/help/matlab/ref/mldivide.html.

[22] D. Griffiths and D. Higham, *Numerical Methods for Ordinary Differential Equations: Initial Value Problems*. Springer, 2010.

[23] *MATLAB. (2020)*. Natick, Massachusetts: The MathWorks Inc., 9.9.0.1524771, R2020b.

[24] *Penn State, Institute for computational and data sciences*. [Online]. Available: https://www.icds.psu.edu/computing-services/.

[25] J. Song *et al.*, "Dynamic modeling of cascading failure in power systems", *IEEE Trans. Power Syst.*, vol. 31, no. 3, pp. 2085–2095, 2016.

[26] N. R. Chaudhuri, S. Ray, R. Majumder, and B. Chaudhuri, "A new approach to continuous latency compensation with adaptive phasor power oscillation damping controller (pod)", *IEEE Transactions on Power Systems*, vol. 25, no. 2, pp. 939–946, 2010.

[27] J. W. Stahlhut, T. J. Browne, G. T. Heydt, and V. Vittal, "Latency viewed as a stochastic process and its impact on wide area power system control signals", *IEEE Transactions on Power Systems*, vol. 23, no. 1, pp. 84–91, 2008.

[28] H. Wu, K. Tsakalis, and G. Heydt, "Evaluation of time delay effects to wide-area power system stabilizer design", *IEEE Transactions on Power Systems*, vol. 19, no. 4, pp. 1935–1941, 2004.

[29] D. Dotta, A. S. e Silva, and I. C. Decker, "Wide-area measurements-based two-level control design considering signal transmission delay", *IEEE Transactions on Power Systems*, vol. 24, no. 1, pp. 208–216, 2009.

[30] S. S. Yu, T. K. Chau, T. Fernando, and H. H.-C. Iu, "An enhanced adaptive phasor power oscillation damping approach with latency compensation for modern power systems", *IEEE Transactions on Power Systems*, vol. 33, no. 4, pp. 4285–4296, 2018.

APPENDIX

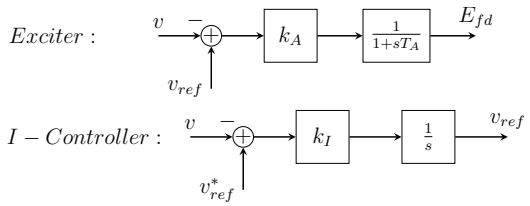

Figure 15: Top: Static exciter model. Bottom: Integral-Controller model. When OPC is active, $v^*_{ref} = v^*_{Gen}$, where v^*_{Gen} is an element of the vector $\mathbf{v^*_{Gen}}$.

Sina Gharebaghi (S'17, S'20) received the B.Sc. degree in Electrical Engineering from Urmia University, Urmia, Iran, in 2016 and the M.Sc. degree in Electrical Engineering from the Sharif University of Technology, Tehran, Iran, in 2018. He received his Ph.D. degree in Electrical Engineering from The Pennsylvania State University, University Park, PA in 2023. His research interests include power system dynamics and stability, cascading failures, and power flow analysis.

Nilanjan Ray Chaudhuri (S'08-M'09-SM'16) received the Ph.D. degree in power systems from Imperial College London, London, UK in 2011. From 2005 to 2007, he worked in General Electric (GE) John F. Welch Technology Center. He came back to GE and worked in GE Global Research Center, NY, USA as a Lead Engineer during 2011 to 2014. Presently, he is an Associate Professor with the School of Electrical Engineering and Computer Science at Penn State, University Park, PA. He was an Assistant Professor with North Dakota State University, Fargo, ND, USA during 2014-2016. He is a member of the IEEE and IEEE PES. Dr. Ray Chaudhuri is the lead author of the book Multi-terminal Direct Current Grids: Modeling, Analysis, and Control (Wiley/IEEE Press, 2014). Dr. Ray Chaudhuri was the recipient of the National Science Foundation Early Faculty CAREER Award in 2016 and Joel and Ruth Spira Excellence in Teaching Award in 2019.

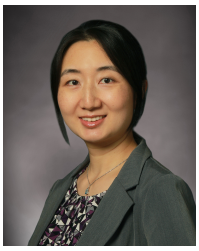

Ting He (SM'13) is an Associate Professor in the School of Electrical Engineering and Computer Science at Pennsylvania State University, University Park, PA. Her work is in the broad areas of computer networking, network modeling and optimization, and statistical inference. Dr. He is a senior member of IEEE, an Associate Editor for IEEE Transactions on Communications (2017-2020) and IEEE/ACM Transactions on Networking (2017-2021), and an Area TPC Chair of IEEE INFOCOM (2021). She received multiple Outstanding Contributor Awards from IBM, and multiple paper awards from ITA, ICDCS, SIGMETRICS, and ICASSP.

Thomas F. La Porta (F'02) is the Director of the School of Electrical Engineering and Computer Science and Penn State University. He is an Evan Pugh Professor and the William E. Leonhard Chair Professor in the Computer Science and Engineering Department and the Electrical Engineering Department. He received his B.S.E.E. and M.S.E.E. degrees from The Cooper Union, New York, NY, and his Ph.D. degree in Electrical Engineering from Columbia University, New York, NY. He joined Penn State in 2002. He was the founding Director of the Institute of Networking and Security Research at Penn State. Prior to joining Penn State, Dr. La Porta was with Bell Laboratories for 17 years. He was the Director of the Mobile Networking Research Department in Bell Laboratories, Lucent Technologies where he led various projects in wireless and mobile networking. He is an IEEE Fellow, Bell Labs Fellow, received the Bell Labs Distinguished Technical Staff Award, and an Eta Kappa Nu Outstanding Young Electrical Engineer Award. He also won two Thomas Alva Edison Patent Awards. His research interests include mobility management, signaling and control for wireless networks, security for wireless systems, mobile data systems, and protocol design. Dr. La Porta was the founding Editor-in-Chief of the IEEE Transactions on Mobile Computing. He served as Editor-in-Chief of IEEE Personal Communications Magazine. He has published numerous papers and holds 39 patents.